THE PENNSYLVANIA STATE UNIVERSITY
SCHREYER HONORS COLLEGE

DEPARTMENT OF AEROSPACE ENGINEERING
AND ENGINEERING SCIENCE AND MECHANICS

AN EVALUATION OF COMPUTATIONAL METHODS TO MODEL LARGE DROPLET BREAKUP

JASON ERIC TURNER

SUMMER 2017

A thesis
submitted in partial fulfillment
of the requirements
for baccalaureate degrees
in Aerospace Engineering and Engineering Science
with interdisciplinary honors in Aerospace Engineering and Engineering Science

Reviewed and approved* by the following:

Michael Kinzel
Thesis Supervisor
Research Associate, The Applied Research Laboratory

Jonathon Pitt
Thesis Reader
Assistant Professor of Engineering Science and Mechanics

George Lesieutre
Honors Adviser
Professor and Head of Aerospace Engineering

Judith A. Todd
Department Chair
P. B. Breneman Chair and Professor of Engineering Science and Mechanics

* Signatures are on file in the Schreyer Honors College.

ABSTRACT

Ice accretion on aircraft has been, and remains, a long-standing problem in the safe operation of flight vehicles. Ice can cause structural damage when ingested in engines and ruins the aerodynamic properties of lifting surfaces when it attaches to them. Ice accretion is typically simulated using a large scale model of an aircraft, or wing, with droplets treated as a dispersed phase. The dynamics of water droplets in the atmosphere are, thus, approximated with models. These models are tuned to match experimental data from in-flight and wind tunnel tests. Historically, icing from water droplets up to 50 micrometers in Mean Volumetric Diameter (MVD) has been considered. However, safety concerns have risen over the presence of droplets exceeding this size. Supercooled Large Droplets (SLD) are a class of droplets exceeding the 50-micrometer MVD limit. Increased droplet diameter complicates the physics of droplet deposition and breaks some of the assumptions enforced in models. This work attempts to provide a means of investigating the physics of an individual droplet, belonging to SLD regime, as it approaches a body in the most computationally efficient manner possible. A Galilean transformation is employed to isolate an individual droplet from a full model. Streamline data for this droplet is collected and then used as an input for an isolated droplet in a compact fluid domain. The droplet inside this domain is captured using a Volume of Fluid formulation of the Navier-Stokes equations. Early results suggest that assumptions of the stability of large droplets is not as certain as previous literature has suggested. This process can be used in any scenario where it is possible to capture a droplet streamline from an averaged data set.

TABLE OF CONTENTS

LIST OF FIGURES

LIST OF TABLES

Chapter 1

Introduction and Background

Section 1.1: Icing History and Supercooled Large Droplets

Catastrophic aircraft icing is a serious risk in flight vehicle operation. Icing on aircraft can reduce efficiency of flight, damage onboard turbomachinery, reduce lifting capacity of wings, and consequently, raise the stall speed of the aircraft. These risk factors have spurred decades of research and innovation in the field of icing. To pass federal safety requirements, modern transport aircraft must meet the Federal Aviation Regulations (FAR). Part 25 Appendix C of this document details a band of common icing conditions and mandates that aircraft retain certain aerodynamic properties when operating in those conditions. General aviation aircraft may not have to meet this criterion, but all aircraft manufacturers that wish to have their aircraft certified for flight in icing conditions must meet these standards. Within the description of icing conditions, a specific range of droplet size and temperature is detailed.

The most extreme droplet described in the FAR–that is to say, the droplet most capable of producing icing–is often described as the "Appendix C droplet". Appendix C droplets are of a maximum 50 microns in diameter, and at the freezing point of water at 1 atmosphere of pressure. Droplets are primarily characterized by these two numbers, Mean Volumetric Diameter (MVD) and internal temperature (and occasionally freezing fraction if they are subcooled). However, Appendix C droplets have been shown to not represent the totality of icing conditions aircraft may face. A new, more hazardous set of droplets has been measured in flight. This new class, known as Supercooled Large Droplets (SLD), is a potent combination of large MVD and subcooled internal temperature. These droplets approach raindrops in terms of diameter, and like raindrops they are completely in a liquid state. Despite their liquid state, experimentally measured droplets in the atmosphere have had internal

temperatures ranging down to -37.5℃ [1–3]. The combined size and temperature of these droplets poses a serious icing risk to aircraft operating in a weather system with SLD.

In 1994, a twin-engine turboprop commuter aircraft (ATR 72) crashed in Roselawn, Indiana while traveling a route between Chicago and Indianapolis. The National Transportation Safety Board issued a statement of "probable cause" naming ice accretion aft of the wing de-icing system as the primary factor in the acciden[4]t. While the aircraft did have a pneumatic de-icing system that was certified under FAR Article 25 Appendix C, the system failed to protect the wing from catastrophic ice accretion. In fact, as the NTSB commented in their "probable cause" [1] statement, the ice accretion occurred behind the de-icing system, outside the protected area. The region of protection for an aircraft wing is set to provide protection against icing from water droplets defined by the FAR 25 Appendix C definition. It was theorized then that droplets outside of this definition must have caused the incident. These larger droplets have the potential to impinge either directly or indirectly beyond the protected area. This accident, and the potential for future accidents of this nature has motivated the study of the atmospheric conditions capable of capable of sustaining large, cold droplets. The European Aviation Safety Administration (EASA) outlined Certification Standard (CS) 25, an Acceptable means of Compliance (AMC), which covers larger cloud-borne water droplets. The standard outlines two categories of large droplets: freezing drizzle (MVD less than 500 microns, greater than 50 microns) and freezing rain (MVD greater than 500 microns)[3]. Moving from the atmospheric sciences to icing literature, when droplets are cooled below the freezing point (but remain liquid due to the lack of a nucleation site) they are referred to as super-cooled. If they are of sufficient MVD, then they belong to the aforementioned class of Supercooled Large Droplets.

Icing on aircraft has been a long-standing problem. The first real mention of icing as a problem for flight vehicles (at least to this author's knowledge) was in reference to early airmail flights between New York and Chicago. On the subject of the hazards of in flight ice accretion, the then superintendent of

[1] "Probable Cause" used in a technical/legal sense here

National Air Transport Inc.–the airline that would eventually become United Airlines–Wesley L. Smith writes in his 1929 article to the Monthly Weather Review, "By coating our planes with ice… the plane will actually fall out of the air if the pilot has not been wise enough to land before this moment arrives." [5] Smith was an airmail pilot in the early days of the profession. The icing conditions he and other airmail pilots experienced crossing the Kittatinny Mountains were the original motivation behind icing research. Smith himself crashed into a mountain in 1920. Surviving this, he continued on as an airmail pilot before transitioning to industry where he would write the aforementioned article.

Airmail routes between New York and Chicago are now far less hazardous, but the perils of icing remain. The National Advisory Committee for Aeronautics (NACA) led some of the original scientific testing in ice accretion[6]. The NACA's construction of a refrigerated wind tunnel in 1929 was the first of its kind and paved the way for future research efforts in ice accretion experimentation. Despite all of the research in the field, the central question implicitly asked by Smith in his article remains: How can engineers prevent crashes caused by a buildup of ice on aircraft?

Some of the world's best engineers have tackled this question and produced many partial solutions. Most modern commercial and military aircraft have deicing systems capable of protecting the aircraft from all but the most severe icing conditions. Additionally, meteorologists can now predict which weather systems pose a risk to aircraft operating in the area.[1–3] Aerodynamicists also understand how ice accretion affects aircraft performance, and can estimate the size an ice growth can reach before it poses a serious risk to the operation of the vehicle. Beyond the expansion of laboratory knowledge of the subject, hours of inflight experience has accumulated and tactics for avoiding or handling ice accretion are now known. There is however a gap in all of this knowledge. This gap is the ability to *predict* what the actual icing limits of an aircraft are. Alternatively, stated as a question: Can an engineer know the precise set of droplet conditions that will down an aircraft, where less severe droplets outside of this set of conditions will only deteriorate the aircraft's performance? This gap is the continuing question in the field. The present work seeks to help advance an answer to this question by providing a tool to answer the

necessary, but not sufficient[2] question: What happens to a water droplet when it impacts a body? A key argument in the present work is that this question is too complex in the SLD regime to be precisely addressed with current experimental methods and their resulting non-dimensional relationships and concepts such as Critical Weber Number. SLD behave notably different than Appendix C droplets as they impinge on a body.

Section 1.2: Current Tools for Understanding and Predicting Ice Accretion

Advanced computational tools have been developed to answer the question posed above. One of the first and perhaps most notable computational tools is the LEWis ICE accretion program (LEWICE).[7] LEWICE is a computational tool used to couple fluid dynamics and freezing computational models together. This program simulates flow around a body in icing conditions, and then attempts to predict the ice shape produced as a result of these icing conditions. This process has four key stages: 1) Flow field calculation 2) Particle trajectory and impingement computation 3) Thermodynamic and ice growth calculations 4) Modification of body geometry to account for ice growth. A fifth stage is the incorporation of de-icing system effects, although not all icing solvers have this functionality. LEWICE has been extensively validated for the most prevalent icing conditions (Appendix C droplets). This methodology is highly efficient, and highly accurate.

In addition to LEWICE, several different simulation software developers have produced tools for predicting ice shapes. They each have their own slight variations on this method, but for the most part produce similar results. Several popular tools are: FENSAP-ICE produced by Ansys, the Eulerian-Eulerian Icing model used in CFD++ produced by Metacomp Technologies[8], and the Dispersed Multiphase model coupled with the Freezing-Boiling model in STAR-CCM+ produced by CD-adapco.

[2] Not sufficient by a large margin it should be noted.

All of these models construct some form of multiphase interaction between the primary and secondary phases in the system. Primary and secondary here refer to the surrounding fluid, and the material suspended in that medium. In the context of icing, the primary phase is air, and the secondary phase is water/ice crystals. These two phases are captured by one of two common frameworks: Eulerian-Lagrangian or Eulerian-Eulerian. These names refer to the numerical reference frame placed on the primary and secondary phases respectively. These models will be explained in further detail in the "Methods" section of this document.

Section 1.3: Current Methodology for Researching Droplet Impingement

Subsection 1.3.1: Experimental Techniques and Results

The large size of SLD makes it difficult to produce stable droplets in laboratory environments. Traditional high-speed horizontal icing wind tunnels must be tuned to slowly accelerate entrained droplets up to the freestream velocity of the flow. If large droplets are inserted into a sharp crossflow, they will prematurely breakup. If they survive the shock of the initial crossflow, then they are accelerated up to the freestream velocity of the tunnel. This acceleration inevitably deforms the droplets and consequently distorts the physics of the resulting deposition. Vertical wind tunnels (relying on gravity as opposed to a compressor) do not artificially distort the droplets as they approach the test section, but cannot simulate representative flight conditions in the way that horizontal wind tunnels can. Namely, they can only model an uncurved droplet streamline. Most early droplet breakup experiments were created to understand combustion, and thus employed a nozzle to produce droplets injected into a quiescent fluid[9]. Pilch and Erdman were primarily interested in liquid-metal cooled fast breeder reactors[10]. As such, they evaluated experiments wherein droplets of liquid metal were observed breaking up in water and alcohol. They claim

that for equivalent Weber number, liquid-liquid and liquid-gas interactions are the same, but also go on to qualify this claim as holding for a limited range of other non-dimensional numbers[10].

A key advantage of horizontal wind tunnels is their ability to directly enforce dynamic similitude with flight conditions. Vertical wind tunnels make a similar assumption to the one made by Pilch and Erdman to achieve dynamic similitude. Gravity is the only driving force on droplets in the tunnel, so the droplets are often far larger in MVD than the droplets atmospheric studies have been able to actually locate and measure. The size disparity is then used to produce critical breakup Weber Numbers on par with the smaller droplets used in horizontal tunnels[11].

When considering the flow of a droplet, the balance of surface tension and inertia is a key physical parameter. This balance can be measured using the Weber Number, which is defined as:

$$We = \frac{\rho v^2 l}{\sigma}$$

We represents the ratio of the inertial forces tearing the droplet, to the surface tension that attempts to maintain droplet cohesion. Critical Weber Number is a means of describing a flow condition before which a droplet is stable, and after which the droplet begins to decompose into two or more smaller droplets.

Early testing from Pilch and Erdman outlined six different mechanisms for droplet breakup, segregating them based on their Weber Number[10]. Figure 1 below is copied directly from their work.

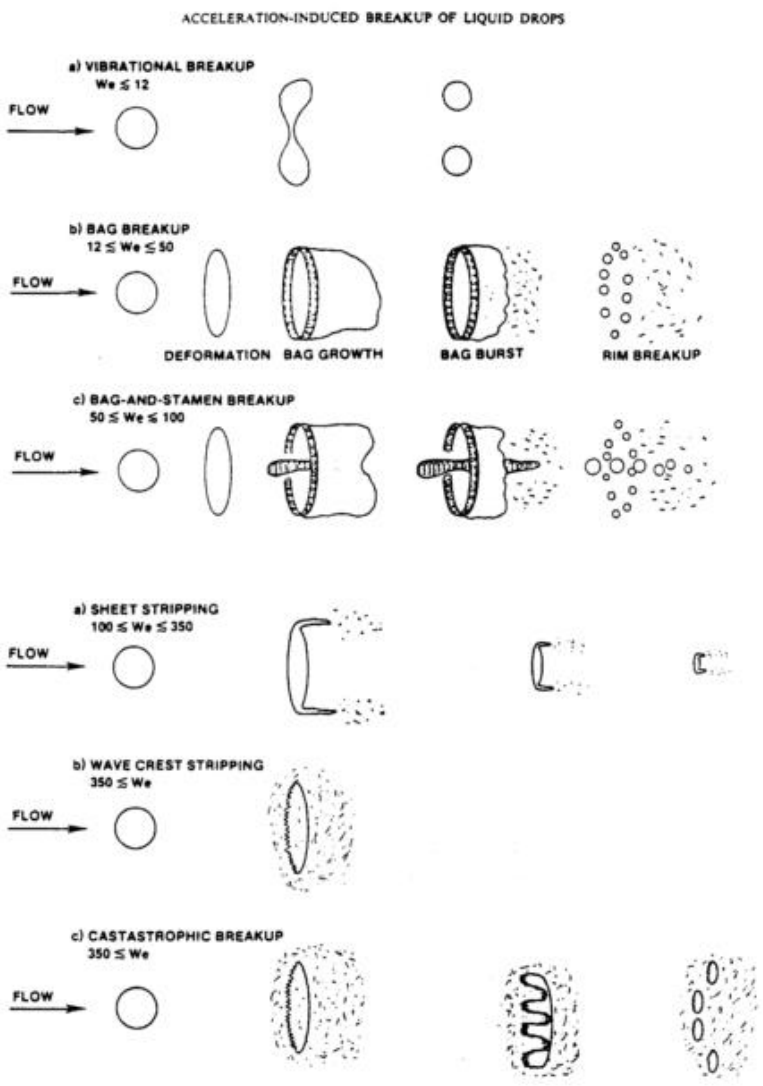

Figure 1. Breakup mechanisms.

Figure 1: Droplet Breakup Regimes

These six mechanisms are defined by a range of *We*. The six regimes are vibrational, bag, bag-and-stamen, sheet stripping, wave crest stripping and catastrophic breakup. These breakup mechanisms describe how a droplet will breakup for a give flow condition. Higher *We* indicate more violent flow conditions. While a droplet falling slowly may eventually vibrate apart, a droplet hit by a shockwave will experience catastrophic breakup. Subsonic flight vehicles are most likely to experience the first three breakup regimes. Critical Weber Number is the number separating vibrational breakup from bag breakup.

It is commonly considered the point after which the inertial forces tearing at the droplet are stronger than the surface tension forces holding the droplet together. Thus when a droplet's *We* exceeds the critical *We*, breakup is imminent. This is somewhat of a misnomer however, droplets can experience vibrational breakup at any *We*.

Further testing has not observed any other distinct breakup mechanisms, but has segregated droplets using different criteria including the Ohnesorge and Bond numbers. A fundamental problem with this approach of classification is that every experiment is still prone to the same methodology errors mentioned earlier. Pilch and Erdman even cite disagreement between researchers before them, emphasizing inconsistent methods of quantifying breakup time. One strong conclusion made by many previous researcher that the present author is less convinced of is that a critical Weber Number (or Bond, or Ohnesorge, what have you) even exists. All of these numbers fail to encapsulate all of the complicated physical mechanisms at work. This critical number is thought to demark the boundary between stable and unstable droplets. Some authors say it is equal to 12, whereas others say it equal to 13. A seemingly trivial difference, but that is still a variation of 8%. This author believes at best, a roughly defined range of stability is the most accurate result available.

Experimentalists[12] have long struggled with imaging droplets during experiment. Often, horizontal wind tunnels seed droplets into the flow in the converging section of the tunnel to aid in their acceleration, while their imaging systems are focused on the leading edge of the test body. This restriction in field of view means that droplets that have broken up prior to entering the recording area with the test body must be thrown out of the experimental data as outliers[13]. In the view of this author, that selection has a strong possibility of introducing artificial breakup properties into droplet dynamics. It seems reasonable to think that the droplets that are discarded from the experiment were those whose initial geometry deformations were most unstable. Thus droplets included in experimental results are those most stable, thereby moving critical breakup Weber Number beyond what is physically realizable during inflight conditions. A numerical approach may provide a solution to this problem of implementation.

Subsection 1.3.2: Numerical Techniques for Researching Droplet Dynamics and Results

An early example of numerical modeling of droplets is the work of J.K. Dukowicz (1980)[9] . In his paper he created a numerical model for droplet-entrained flows. His early work in multiphase flow theory produced many meaningful results, but full realization of his model was limited at the time due to a lack of computational resources. The model simulates two-way interaction, or coupling, between the primary phase: air, and the secondary droplet phase dispersed in the medium. This coupling takes the form as an interaction model between the dispersed and continuous phases. The goal of the coupling is to capture the physical effects of the interface (also known as a free surface) on the flow. This interface transfers momentum between the two phases. In Dukowicz's model, the coupling is referred to as a two way couple because the equations defining momentum transfer across the free surface effects the flow of both phases of matter in the domain. The model quantifies the effects of displaced air due to the presence of the droplet, and the momentum interchange from the particles back to the surrounding fluid. An important computational engineering note is that this coupling is computed within the time step, thus the computational cost of the model is highly sensitive to the temporal discretization required to resolve the inter-phasic equations. An alternative to a two way couple, is a one way couple wherein momentum is only transferred down length scales to the entrained droplets, and not up from the droplet phase to the surrounding phase. While this is a simplification of the real physics, it can cut computational costs while introducing a minimal level of error for specific classes of flows. Dukowicz's model would later be categorized into a series of multiphase modeling approaches designated Eulerian-Lagrangian models. This name refers to the modeling approach applied to each of the two phases. The air flow around a body is computed using a fixed Eulerian mesh, whereas the droplets entrained in the flow are modeled using Lagrangian equations for the dynamics.

While each Lagrangian droplet can have any value set as its MVD, a key and strong assumption made in the model is that this diameter is invariant. The droplets are incapable of experiencing breakup or coalescence. This assumption comes from the idea that droplet entrained flows are 'sparse'. Droplets are

viewed as discrete entities, effectively alone in their environment. Their inter-particle interactions are, quite literally, nonexistent. The entire model restricts physical interaction entirely to the liquid-gas interactions; no liquid-liquid collisions are allowed. Furthermore, the assumption that droplets don't breakdown was invoked at the time because researchers didn't have a good model for computing breakup. This would change however.

Reitz[14] (in 1987) would advance the model of Dukowicz by successfully implementing a scheme for modeling the stochastic nature of droplet breakup and coalescence. His work was used for a different class of simulation however. Instead of solving for flow over a generic body, Reitz was interested in jet flows injected into a quiescent medium[3], a flow in which he could apply inviscid flow theory. O'Rourke and Amsden[15] created the Taylor Analogy Breakup Model (TAB) in 1987, a model more applicable to the Eulerian-Lagrangian framework pioneered by Dukowicz. This model took the stochastic model created by O'Rourke in a previous publication, and used it to create a Lagrangian breakup model capable of predicting secondary breakup of droplets injected and diffusing in a quiescent fluid. Similar to Reitz, the model was originally created to simulate diesel injection into engine cylinders. The work was strongly motivated by findings that suggested secondary breakup of droplets in the combustion chamber dominated the energy of combustion, and the resulting power output of an engine. Spray equations had already been derived to predict the resulting droplet diameter produced in a spray, but this new TAB model was capable of tracking those droplets once they had~~'d~~ been sprayed, and then predicting their secondary decay.

The addition of the Reitz and TAB models to the Eulerian-Lagrangian framework created by Dukowicz was an incredible step forward, but still, multiphase modeling was constrained to cases where the model was applicable. Ultimately, the Eulerian-Lagrangian formulation is limited by its mathematical construction. Every new computational particle injected and tracked in the simulation directly increases

[3] Specifically, Reitz was interested in diesel injectors in engines.

the computational cost. Simulating atmospheric flows, particularly those relating to icing conditions, is effectively impossible. It would take an immense amount of computational power to faithfully simulate full, multiphase icing conditions around a wing, let alone an entire aircraft. A second key limitation relating to the underlying mathematics of Eulerian-Lagrangian models is the inherent separation they impose on the two phases. Dukowicz's model does couple both phases of flow together. This is accomplished with an equation, which captures buoyancy and drag on the fluid continuum, but this coupling is incomplete. The fine details of the free surface are not modeled. Furthermore, the governing equations for the two phases of flow are solved separately from each other. The bulk airflow around the body is solved on an Eulerian mesh that is invisible to the dispersed droplet phase. The two phases are only interacting with each other through a numerical interface, as opposed to being directly computed, together, on the same domain.

These limitations of the Eulerian-Lagrangian framework led to work in a new framework for multiphase flow simulation, Eulerian-Eulerian models. Models of this type capture the dispersed droplet phase in the mesh, and compute the effects of the multi-phasic interactions everywhere in the domain. At the inception of droplet modeling, both Eulerian-Lagrangian and Eulerian-Eulerian frameworks were developed, but early success in modeling diesel injectors favored Eulerian-Lagrangian frameworks. This was because of the early droplet breakup models like the TAB and Reitz models were developed in Eulerian-Lagrangian frameworks. Eulerian-Eulerian frameworks are preferable to larger domains as they can scale to a large number of disperse droplets more easily, whereas Eulerian-Lagrangian frameworks increase in cost for every new fluid particle. This increase in scalability ~~doesn't~~does not come without cost. Until recently[8], it was difficult to model breakup in an Eulerian-Eulerian framework, and transport equations for the dispersed phase required a singular, fixed droplet diameter. If an engineer wished to allow for the breakup of droplets, each new droplet size behaved as if there were an entire other phase of matter in the fluid domain. Likewise, the droplets have to obey the previously stated assumption of 'disperse-ness'; interactions between droplets are not directly simulated. Kim, Bachchan and Peroomian[8]

(2016) have detailed one of the most up to date methods for simulating droplet flows in an Eulerian-Eulerian framework. Their tool is capable of computing an evolving value for the number density of water droplets per grid cell. Using some initial experimental work from authors like Pilch and Erdman[10], Kim, Bachchan and Peroomian have tuned their tool to agree with existing theory and empirical evidence. Namely, as the computational cost of additional droplet sizes is great, Kim, Bachchan and Peroomian employ the idea of a Critical Weber Number to determine the stability condition as their number density equation evolves throughout the flow field.

Reitz[14], in his droplet breakup modeling paper cites the aforementioned vertical wind tunnel tests (in section 1.3.1) as confirmation of the Weber Number regimes first outlined by Pilch and Erdman[10], despite what appears to this author to be a statistically significant variation in measured critical Weber Number. The variation in the data seems to promote the idea that while the ranges originally put forward by Pilch and Erdman, are more guidelines than strict physical laws. Pilch and Erdman[10] actually discuss an experimental method dependency on the precise value for Critical Weber Number, specifically stating that gradually accelerated droplets do not experience breakup in the same fashion as those directly impacted in a jet crossflow[4]. The Critical Weber Number for these droplets w~~e~~as~~re~~ observed as higher than those measured for droplets struck by a jet crossflow. For a long time this problem in droplet modeling has gone ignored as the variation in critical Weber Number has far less significance for more conventional small droplets (such as those defined under FAR 25 Appendix C). Small droplets have a higher surface energy to volume ratio (a ratio inversely proportional to Weber number) which anesthetizes them to the higher frequency instabilities that promote breakup in larger droplets (such as SLD). This assumption could mask some of the early breakup processes present in SLD.

In summary, ~~numericists~~ numerical modelers have created empirical and semi-empirical models for simplified droplet geometry mechanisms tuned to match the observed physics. These models either

[4] An environment akin to the atomization nozzles used in diesel injectors.

take a data set and attempt to reproduce the outcome using a small number of independent factors in a purely empirical fashion, or they postulate a first order droplet breakup mechanism and prescribe a tuned formula that produces output which correlates well with a set of experimental data. These models are then solved alongside equations for the surrounding airflow. Some researchers claim to have better models that utilize a different perspective when solving for the motion of the droplet flow, but even this description of the droplet only models the interphasic forces between the dispersed and continuous phases instead of trying to simulate them. At the core, all of the numerics and applied physics applied to droplet breakup has been forced to match experiments. This is all, in essence, fruit of the poisonous tree; all of this work is subject to the same critic leveled against the experimentalist; strong assumptions have been made that are not present in real flows, and the resulting categorizations stand on uncertain footing. Current research (as an example, the work of Jain, Prakash, Tomar and Ravikrishna) is focusing on the high fidelity resolution of an individual droplet. The hope behind this work is that further examination of the breakup process at the sub-micron level can elucidate knowledge about stability and breakup of droplets that can inform models at the macroscale.

Section 1.4: The Role of Present Work

The purpose of this work is to provide a new means of understanding and observing these droplets in a way that experiments cannot reproduce fully. The methods described in this paper are not perfect as they make certain assumptions of the geometry of the droplet, and the scale separation between droplet breakup and droplet motion. The latter assumption even utilizes one of the droplet motion models just criticized as *fruit of the poisonous tree*. There is however one key distinguishing factor of the present work: while the environment around the droplet inherits the artificiality of laboratory experiments, the droplet itself behaves as a “real” droplet. This droplet is not constrained in the way droplets are in a laboratory experiment (except for the symmetry assumption that will be discussed and reviewed later),

and the surface of the droplet is free to deform (as opposed to modeled approaches). The goal of this document is to shed insight onto the validity of the assumptions made in past work, and outline an efficient method of exploring this question further.

It should be stated that this document does not seek to impeach the sizeable amount of experimental data in large droplet dynamics. Instead, a method is proposed for investigating droplets difficult to produce and record experimentally. This in turn is a means of verifying droplet characteristics that have already been measured. The present work is therefore an attempt to provide a means for observing and understanding the fundamental physical behavior of Supercooled Large Droplets, specifically their behavior in the moments prior to impingement.

Chapter 2

Methodology

The key mission of this work is to describe a novel process in modeling the dynamics of large droplets as they approach a wing in such a way that minimizes computational cost, without sacrificing the fidelity in resolution of the complicated physical mechanisms at play in the droplet breakup process. This new model is then used to reproduce experiments from prior authors, as well as project results to tests that have not yet been conducted. These modeled results are then compared against existing theory to qualify their validity and applicability to flight vehicles, and interesting or otherwise peculiar phenomenon are discussed. Recommendations for future work will be included later in this document.

Section 2.1: Process Overview

The proposed simulation procedure consists of two simulation phases. First, a simulation of the flow field seeded with droplets around an airfoil is computed using a relatively straight forward Eulerian Multiphase simulation. This allows for a relatively cheap computation, and geometric changes resulting from ice accretion are ignored. The precise parameters of this simulation are discussed later. The primary mission of this stage is to compute the properties of the flow field a droplet would experience as it approaches a body. These properties are captured at scales similar to that used to simulate flow around the airfoil. For this reason, this portion of the process will be referred to as the "macroscale simulation".

After the macroscale simulation has been conducted, velocity data from the streamline is extracted from the simulation and tabulated. Depending on the tool used to compute the streamlines (and specifically its allocation of memory when running on multiple threads), the data may need to be sorted. Additionally, streamwise values for Weber, Robin, Bond and other important dimensionless parameters are computed. Finally, the time in a Lagrangian reference frame is computed for each discrete position point of the streamline, and the time/slip velocity/droplet velocity data is exported for use in the next phase of simulation. This is discussed in more detail in Section 3.

With the data all collected and sorted, a new simulation can be run on a local region of fluid around a single droplet of interest. This simulation is the most computationally expensive part of the entire simulation, and the fidelity of the mesh here sets the precision of the results. To merely demonstrate the capability of this method, only a simplified axisymmetric simulation was run. The key objective of this phase of the process is to attempt to fully resolve what effect the chosen droplet streamline has on the geometry and breakup characteristics of the droplet. A value for Critical Weber Number and a determination of the breakup mode could be made at this step. This phase will be referred to as the "microscale simulation" in reference to the size of the fluid domain and the length scales on which the surface tension forces act.

The key strength of this method is that it attempts to use the best possible frame of reference at every layer. In a world with infinite computational power, one would simulate a full model of an aircraft in an infinitely fine mesh with remeshing to capture a moving body. This is effectively impossible with current high performance computers. So first a ~~more narrow~~narrower field of view, and an accompanying reference frame shift is made. Instead of a full aircraft, only the wing is investigated; and instead of moving the wing, a Galilean transformation is made by fixing the wing in space (akin to changing the point of observation) and imposing a free stream velocity at the inlet of the domain. Completely resolving individual droplets is still effectively impossible at this level of detail. The desire is to capture as small a domain as possible, just around the droplet and a small volume of air. To get to this, another simplification and change in reference frames is made. A Galilean transformation is made, moving the point of observation from the wing to an individual droplet following a streamline. Here we can narrow the field of view from a length scale roughly equal to the wing chord, to a length scale on par with the droplet diameter. This is a massive reduction in domain scale, and dramatically reduces cell count. Critically though, the boundary conditions on this reduced fluid domain have to match those values from the streamline. The macroscale simulation provides time averaged values for these boundary conditions at discrete points in space. The Galilean transformation from the wing to the droplet requires that the boundary conditions also be converted from discrete data points into a discrete set of inlet conditions at a fixed physical time. The end goal is to represent a fluid element of differential volume traveling along a streamline to a rigid body. The information from the macroscale simulation is fed into the differential volume so that the differential volume (or microscale simulation) only sees a single droplet, a small pocket of surrounding air, and the effects of the multiphase flow comparatively far away from it. As there is no general solution to the Navier-Stokes equations, it is impossible to solve for an infinitely small fluid volume in a flow problem such as this. So mesh fidelity then affects the quality of the streamline data, and the computed physics for a single droplet.

Section 2.2: Droplet Streamline Simulation - Macroscale Simulation

The flow field around the wing is solved over a single cell thick C-Mesh around an airfoil. The STAR-CCM+ Eulerian Multiphase model was solved using the Dispersed Multiphase submodel. This model solves for flow of the primary phase (air) around the airfoil, in conjunction with a model for the flow of dispersed droplets of a fixed diameter. These droplets are treated as hard spherical particles, and their drag physics is approximated using a drag coefficient model.

An important characteristic of this model is that information is transferred only from the primary phase to the secondary phase, and not in the reverse direction. This makes the computation cheaper, but does introduce error, particularly for larger droplets. A more thorough analysis may see benefits from a two-way coupled model. Also, to account for the effects of turbulence the Spalart-Allmaras Turbulence Model[16] was used. This model is particularly well suited for wing flows, and as a one equation model, it remains comparatively cheap.

Convergence is measured using lift coefficient on the airfoil. Both airfoils used in the present analysis are symmetric, so an asymptotic convergence criterion can be created to halt the solution after the simulation has settled on a lift coefficient of zero. From here, any streamline in the flow field can be extracted. To ensure that the droplet impacts a rigid wall, the stagnation streamline is computed by looking for a cell on the wing leading edge with a pressure coefficient of 1, and then integrating backwards to the inlet. The droplet velocity, position in space and relative velocity between the droplet and the surrounding air is then extracted into a table and exported for the next phase in the process.

Section 2.3: Streamline Data Analysis

The droplet velocity, position data and relative velocity data is sorted based on position. This sorts the data into what the droplet experiences as it travels along the streamline. When running the

macroscale simulation on a single core, normally this step is unnecessary, but occasionally when running on multiple threads, the simulation data is not saved sequentially, so sorting becomes necessary.

After sorting the data is then used to compute time along the streamline. The macroscale simulation computes time averaged velocity data at fixed positions, so this has to be converted into time varying velocity data. To accomplish this a simple first order forward finite differencing scheme was employed. Higher order schemes could be used, but the velocity data is all contained at fixed points in space. These points are defined by the mesh cells. A higher order scheme could help when resolving a sharper velocity gradient, but the mesh already accounts for this. As the velocity gradient sharpens near the boundary layer of the wing, the grid resolution also increases. This helps to relax the requirements for interpolation of velocity data from position to position.

An ancillary feature of separating the streamline data from the macroscale simulation is that it allows for the computation of the relevant dimensionless parameters prior to simulating the actual droplet. The macroscale simulation does not account for breakup, instead enforcing a fixed diameter for all of the droplets in the flow. This allows for Weber number to be directly computed from the velocity data. It follows then that the time when the droplet reaches the Critical Weber Number can be computed in advance. A snapshot at this time in the simulation could shed insight into droplet stability, and which vibrational mode is responsible for droplet breakup. Furthermore, physical time values can be associated with each droplet breakup regime. These time values can then be used as a basis of comparison against the actual results from the microscale simulation

Section 2.4: Droplet Simulation - Microscale Simulation

With the time varying inlet condition isolated and organized from the previous phase, a new CFD domain can be constructed using that data. In the hopes of demonstrating this method for the lowest possible computational cost, a 2D axisymmetric domain was constructed. This domain forces radial

symmetry along the central axis of the droplet. The top of the domain is set to be a symmetry plane. A pressure outlet may also be a suitable condition; however, early runs had issues with reversed flow at the boundary when the inlet velocity was nearly zero. On the right hand side of the domain is the flow inlet boundary. This boundary is set to provide a time varying inlet velocity equal to the relative velocity between the droplet and the local air velocity. When the stimulation begins, this velocity is zero, and it is not till the droplet enters the local flow field around the wing that this quantity begins to change rapidly. Smaller droplets follow the airflow more closely, but the larger droplets have more inertia, and thus experience a higher relative velocity prior to impingement. As the initial fractions of a second have little in the way of flow, it is sensible to take the inlet and shift it forward in time such that the relative velocity is no longer minutely small. Not only will this reduce overall simulation time without reducing accuracy, it also helps ensure stability in the simulation. The final boundary condition on the left hand side is a pressure outlet.

In constructing the grid, it is important to maintain cell isotropy and a low level of skewness overall. The droplets can decompose in a number of different modes, and each mode is strongly affected by the local geometry of the free surface. Therefore, the mesh shape can strongly affect breakup patterns. Additionally, the macroscale simulation is not a perfect representation of what happens at the microscale level. In the microscale simulation, droplets are allowed to deform and thus become more ballistic. This tends to mean that they travel laterally throughout the small fluid domain. If the macroscale simulation had a perfect model, the droplet would simply deform in place. To allow for freedom of movement, a region of grid refinement is created at the base of the domain extending forwards and backwards from the center of the droplets initial location.

To model the free surface interface between the droplet and the surrounding air, the Volume of Fluid (VOF) method is used. This method tracks the volume fraction of each phase of matter present in the simulation. In this instance, there are again only two: air and water. The free surface is captured along the grid where volume fraction is between one and zero. One representing that the cell volume contains

entirely air and zero representing that the cell volume contains only water. Cells marking the boundary between the phases have some fractional amount of each phase. Thus their volume fraction lies between zero and one. Properties like density of this two phase material are computed using a volume average. The method is most accurate when this two-phase material is entirely one cell thick along the interface. Additionally, the volume of cells at this interface determines the length scale of resolution the simulation can muster for the free surface. As breakup is strongly dependent on resolving this free surface to the highest possible fidelity, the bulk of mesh resolution is spent on ensuring a high quality mesh around this free surface. A more efficient adaptive meshing approach, like the one employed by Jain, Prakash, Tomar and Ravikrishna[17], can supplement an already highly resolved mesh to either improve resolution further, or reduce cost when fidelity is less important.

The reference frame switch is again the most important feature in this phase of the process, and the entire method. The streamline data has already been processed and converted into a time varying velocity inlet condition from the previous phase. In this phase, that data is used as the boundary conditions for the simulation. Additionally, the governing equations used in the simulation have to be shifted with another time varying condition. This condition corrects the velocity field for the motion of the domain itself. Obviously, directly applying a velocity inlet condition to a droplet will blow the droplet out of the fluid domain, given enough simulation time. To counteract this, the entire domain is constructed in a translating reference frame that has the droplet initially traveling forward with the free stream velocity of the flow field, and decelerating to keep pace with the particle streamline extracted from the microscale simulation earlier. Combined, the relative slip velocity and reference frame velocity applied to the compact microscale fluid domain can determine the system.

As a final note on the number and type of experiment performed, below is a table detailing the exact parameters and outcomes of the experiments.

Table 1: Matrix of Experimentation

Freestream Velocity (m/s)	Droplet Size (microns)	Airfoil
100	50	NACA 0012
100	100	NACA 0012
100	200	NACA 0012
80	473	DBKUP 02
120	2000	DBKUP 02

Section 2.5: Criticism of the Proposed Method

The proposed method yields a relatively high fidelity solution at a fast rate, at least for the size of the computation. Rapid changes in the accelerating flow field are matched by the increasingly refined grid in the macroscale simulation. The method is best suited for scenarios with rapidly increasing Weber Number. A rapidly increasing Weber Number means that the droplets are less prone to vibrational breakup, and bag breakup becomes more likely. The axisymmetric boundary condition imposed in the simulation favors droplet breakup mechanisms that maintain axisymmetry themselves. This is a critical failing. The first breakup mode is heavily suppressed by virtue of the construction of the domain. Only an axially symmetric vibrational breakup is possible. This is not typical for vibrational breakups. As documented by Pilch and Erdman[10], vibrational breakup typically occurs transverse to the flow. At best this is an unfinished and unproven method. A truly three-dimensional case would demonstrate the strengths and weakness of this method more fully.

Chapter 3

Results & Discussion

Section 3.1: Macroscale Simulation

This step in the simulation procedure is the most conventional, and thus there is not much information to glean from this stage. As outlined in the methods section, an NACA 0012 or DBKUP 02 airfoil is placed inside of a domain. A droplet flow is then solved around the wing section. Figure 1 shows the droplet stagnation streamline extracted from the simulation over a section plane displaying the air velocity field around the wing section. This figure serves as an overview of the macroscale simulation process. From the slip velocity streamline, it is clear that the closer a cell is to the body, the higher the slip velocity. This trend is expected as droplets have a higher density than the surrounding air, and thus have more inertia. A similar trend is reversed when the droplets pass through the accelerating regions of flow outside of the stagnation region of the airfoil. There, the droplet velocity is less than the local air flow speed, This trend is expected as droplets have a higher density than the surrounding air, and thus have more inertia. A similar trend is reversed when the droplets pass through the accelerating regions of flow outside of the stagnation region of the airfoil. There, the droplet velocity is less than the local air flow speed.

Figures 2 and 3 display the same slip velocity streamlines over a Weber Number field. This Weber Number field is computed using the initial diameter of provided in the simulation. Recall that for Eulerian-Eulerian simulations without droplet breakup models, the size of the droplet can not evolve over time. So this Weber Number field should not be thought of as a direct computation of Weber Number, but instead the value Weber Number would take on if the droplet decomposed precisely at a given point in the field. The Weber Number field for the DBKUP 02 section is far more jagged than the one around the

NACA 0012 section due to the geometry of the DBKUP 02 airfoil. The DBKUP airfoil was designed to represent the leading edge of a high thickness ratio blade used on either transport airplanes or helicopters. As a result, its stagnation region is much more abrupt than its more streamlined counterpart, the NACA 0012 airfoil. With the streamlines extracted from all of the cases, the data is ready for analysis.

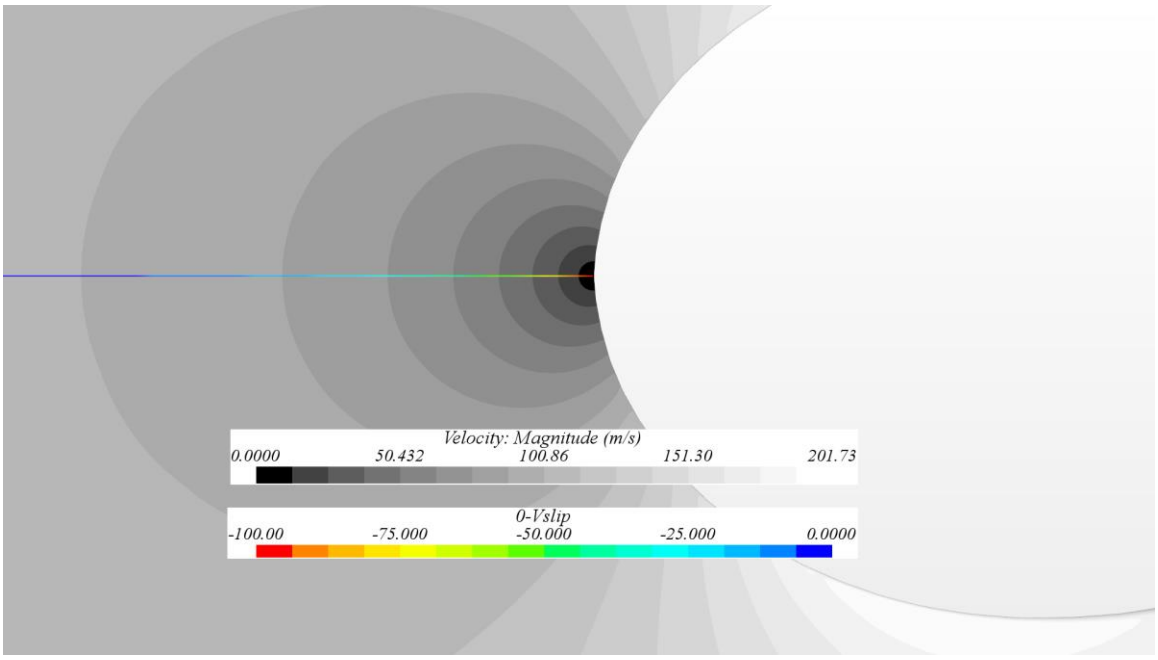

Figure 2: 473 µm MVD Droplet Streamline Over Velocity Field Around DBKUP 02 Section

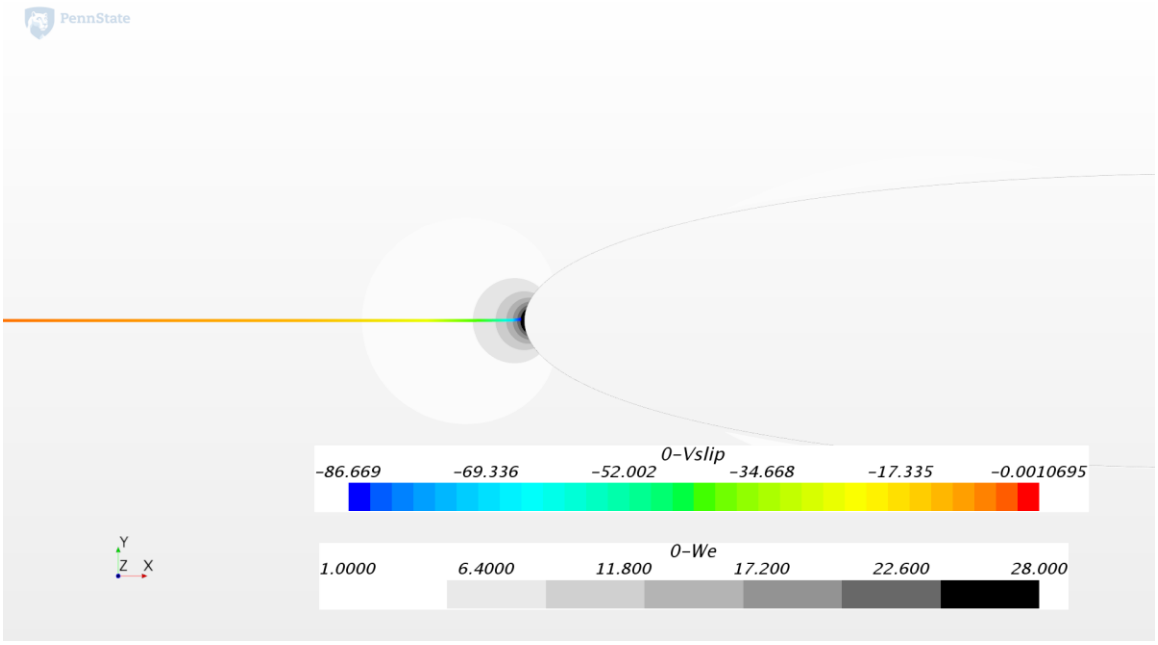

Figure 3: 200 µm MVD Droplet Streamline Over Weber Number Field Around NACA 0012 Section

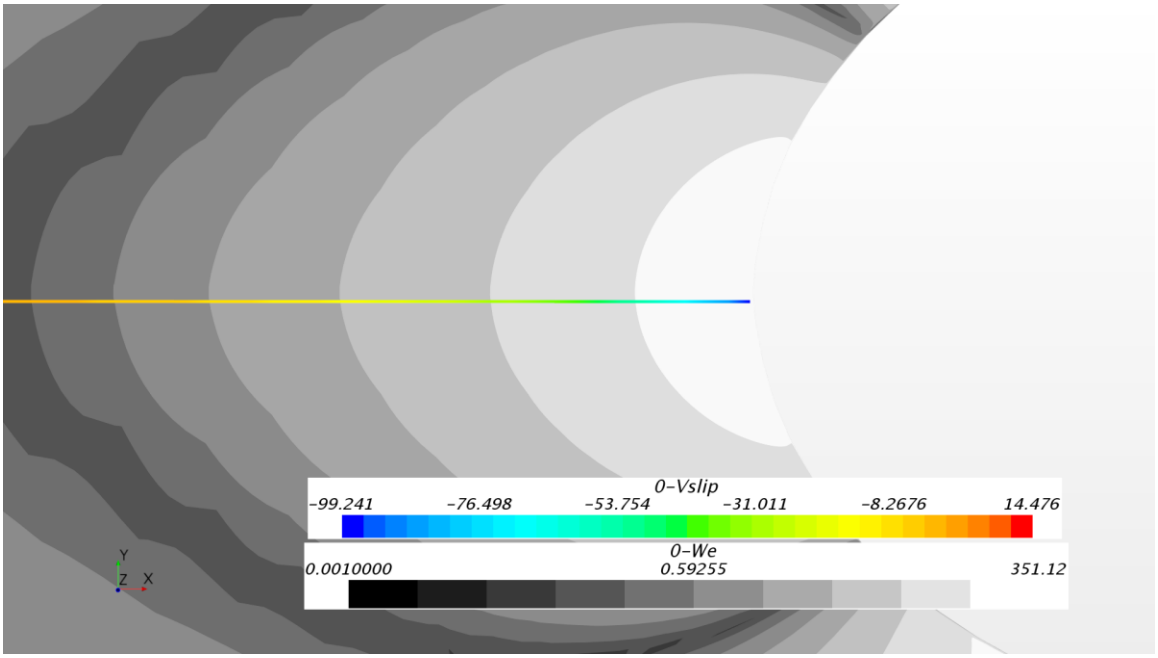

Figure 4: 2000 µm MVD Droplet Streamline Over Weber Number Field Around DBKUP 02 Section

Section 3.2: Streamline Data Analysis

Figures 4-10 highlight various aspects of the streamline data extracted from the macroscale simulation. Figures 4 and 5 display slip velocity along the streamline. This velocity value serves as the basis for several future calculations. We also see in Figure 4 odd rising and falling slip velocity of the 2000 μm droplet. This is actually a result of the initially negative values for slip velocity on the larger droplet. The droplet enters the domain at the same velocity as the rest of the airflow, but maintains this velocity longer than the airflow, and thus has a negative slip velocity that eventually crosses back to positive as the velocity field switches from decelerating to accelerating relative to the droplet. The presence of behavior like this is a problem for the method. Velocity inlet boundary conditions are only suited for specifying flow into the domain at a fixed velocity, not out. To circumvent this issue, an assumption is made that such far field deformations were minimal in scale and would thus not strongly impact the final stability of the droplet. This is a strong assumption that may not hold.

Figures 6 and 7 display how Weber Number evolves over position. This plot is relatively simple and all of its data comes directly from the extracted streamline. Position is measured in distance from the leading edge of the airfoil. Furthermore, the abscissa is given in a log scale. The log scaling is good way for capturing the phenomenon as the extreme slip velocities are only reached just before the leading edge. Also, note the change in the limits on the ordinate axis. The droplets simulated in the NACA 0012 simulation barely reach a Weber Number of 25 at the most extreme. The massive 2000 μm droplet in the strong flow field is capable of reaching an extremely high Weber Number. This is a strong indicator that the droplet will experience a more powerful breakup mechanism.

Prior work has used Bond Number instead of Weber Number to determine criticality. Figures 8 and 9 were included for the sake of completeness and to provide a basis of comparison.

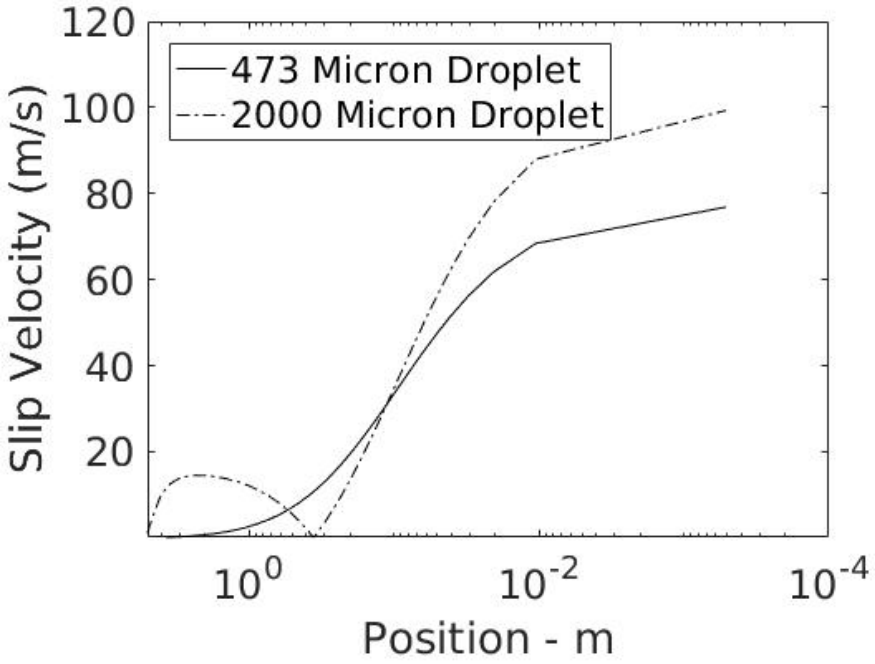

Figure 5: Slip Velocity vs. Distance from Leading Edge of DBKUP 02 Section

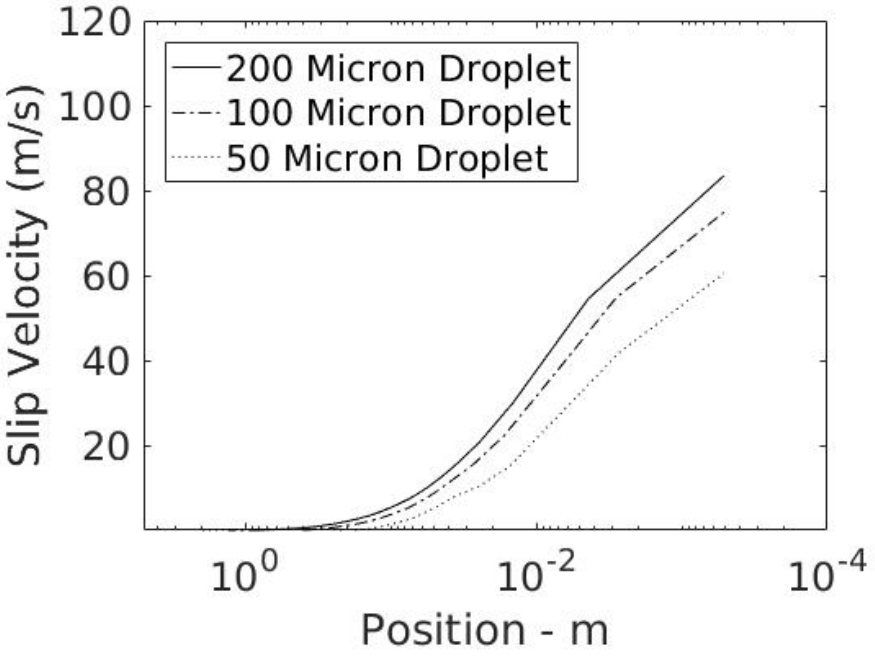

Figure 6: Slip Velocity vs. Distance from Leading Edge of NACA 0012 Section

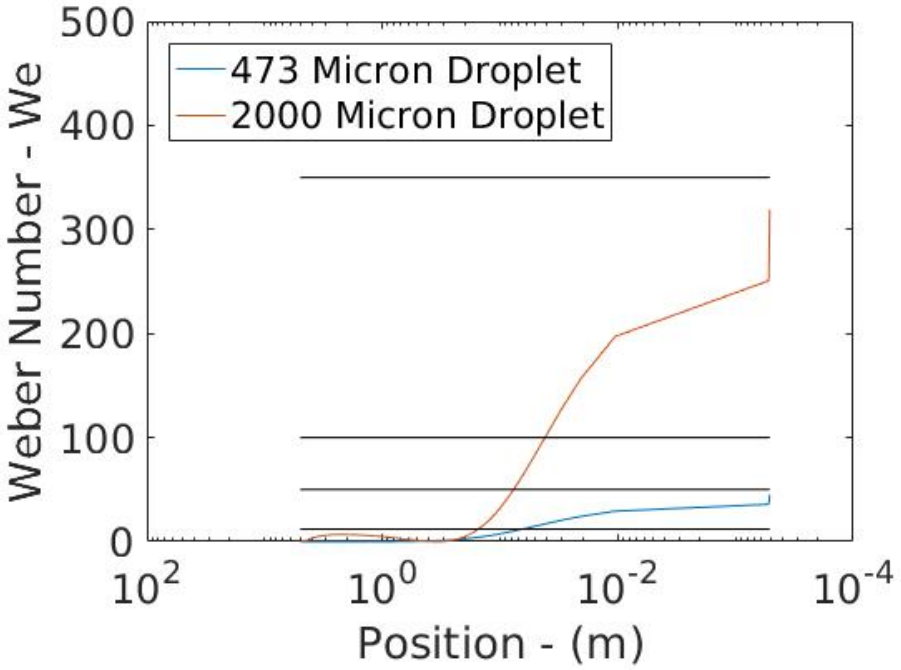

Figure 7: Weber Number for Fixed Diameter Droplet vs. Distance from Leading Edge of DBKUP 02 Section

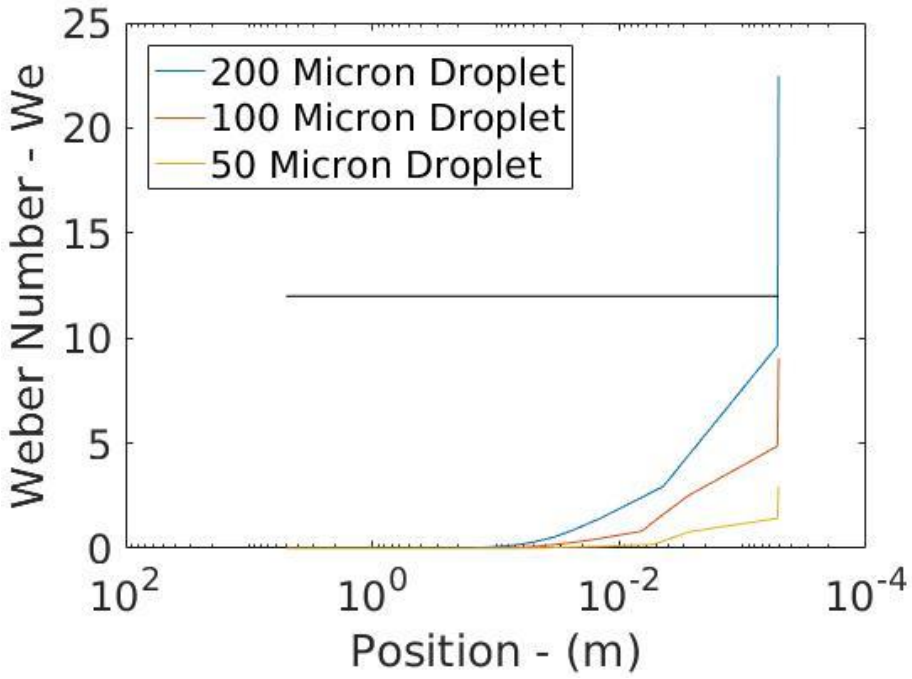

Figure 8: Weber Number for Fixed Diameter Droplet vs. Distance from Leading Edge of NACA 0012 Section

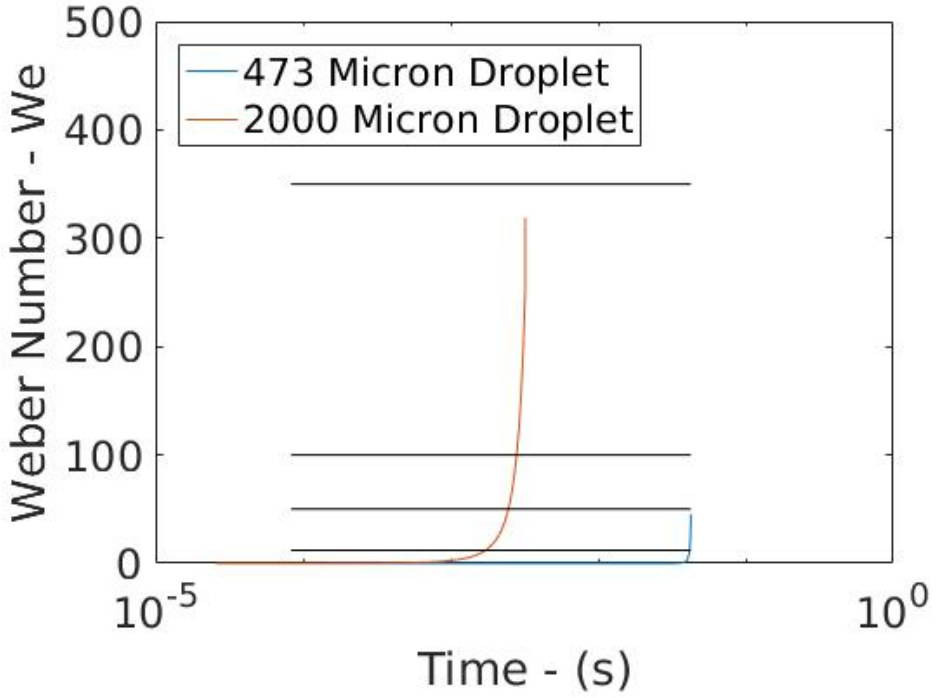

Figure 9: Weber Number vs. Time Along Streamline for DBKUP 02 Section

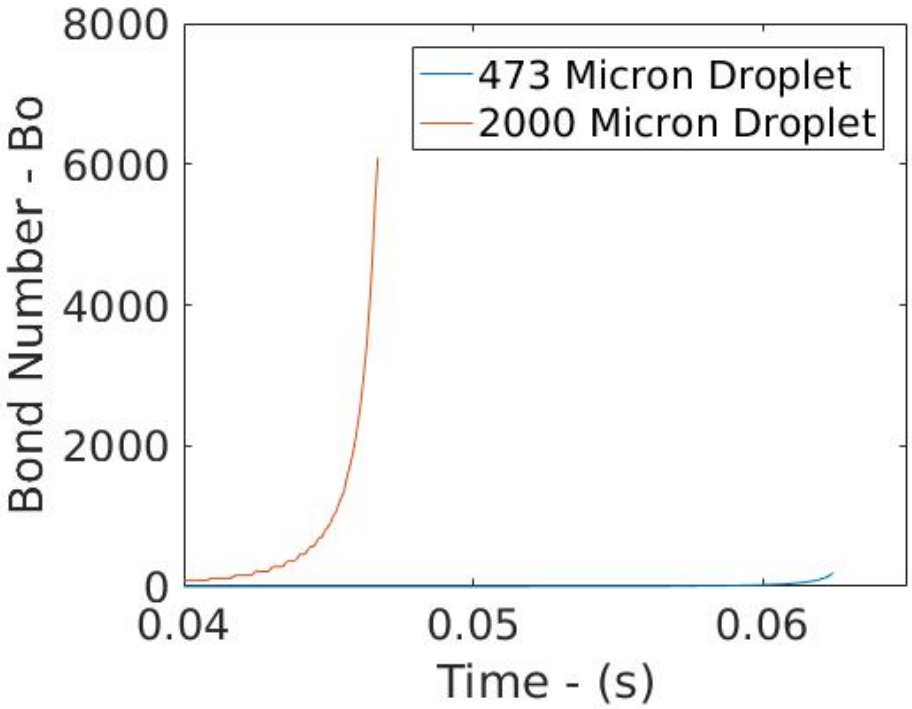

Figure 10: Bond Number vs. Time Along Streamline for DBKUP 02 Section

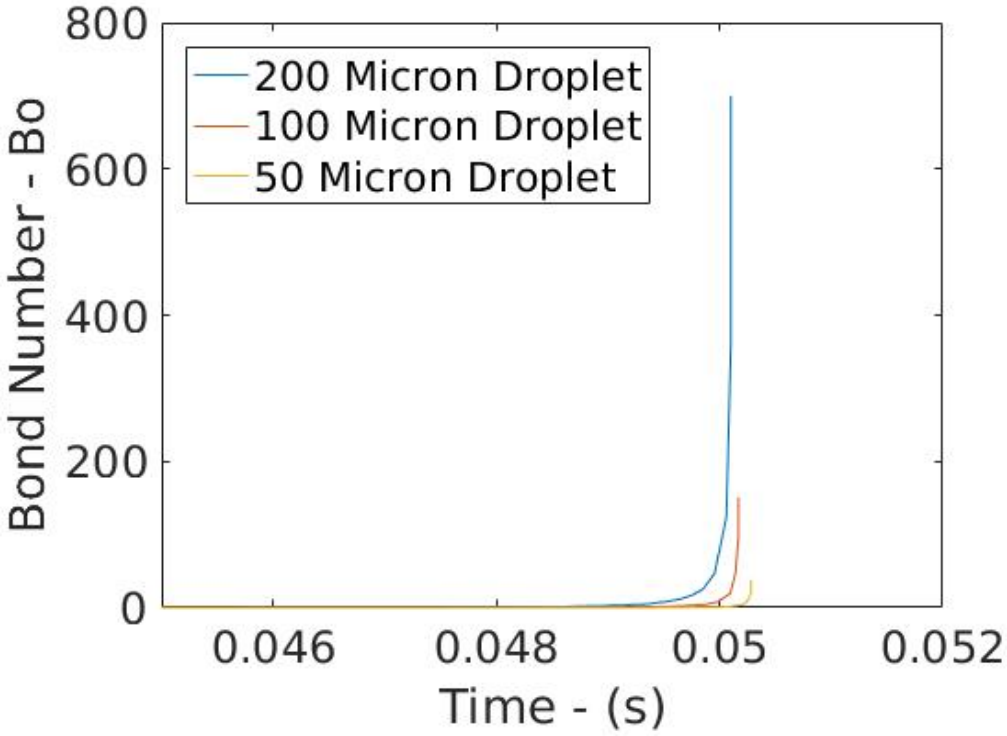

Figure 11: Bond Number vs. Time Along Streamline for NACA 0012 Section

Section 3.3: Microscale Simulation Results

The droplet presented in Figures 12-18 is the same 473 µm droplet in every frame. The figures display the evolution of this droplet over its entire journey till impingement. To improve stability of the simulation, an offset time value of 0.02 seconds was used to increase the slip velocity to roughly 1 cm/s. This value is large enough to ensure stability, but small enough to maintain the assumption that the far field behavior of the droplet is less significant. The droplet can be seen as the colored ball in the center of the domain. A cross section of its shape is shown over the surrounding velocity field. The red through blue colors denote volume fraction of the cells, while the greyscale background shows the velocity field. For volume fraction, red indicates a volume fraction of 1 while dark blue indicates a volume fraction of 0.4. The inner core of the droplets is thus purely water, with an outer layer representing the free surface.

The thickness of this blue layer relative to the red core is a good measure of fidelity. If the blue layer is thin relative to the red core, than the VOF simulation is well within acceptable parameters. In this particular simulation, the droplet resolution starts out fine, but later stages in the simulation leave something to be desired.

Figure 12 shows the droplet early on its path to impingement. The droplet appears to be completely stable. Figure 13 shows some early evidence of vibrational breakup. This may be a misnomer however. Note that the separate lobe is entirely of a low volume fraction. True vibrational breakup would have lobes split off at roughly equal size. The following figures all have the overview of the fluid domain with physical time displayed; a zoomed in view of the droplet itself; and an image taken from Pilch and Erdman[10] depicting the breakup mechanism the droplet is currently experiencing.

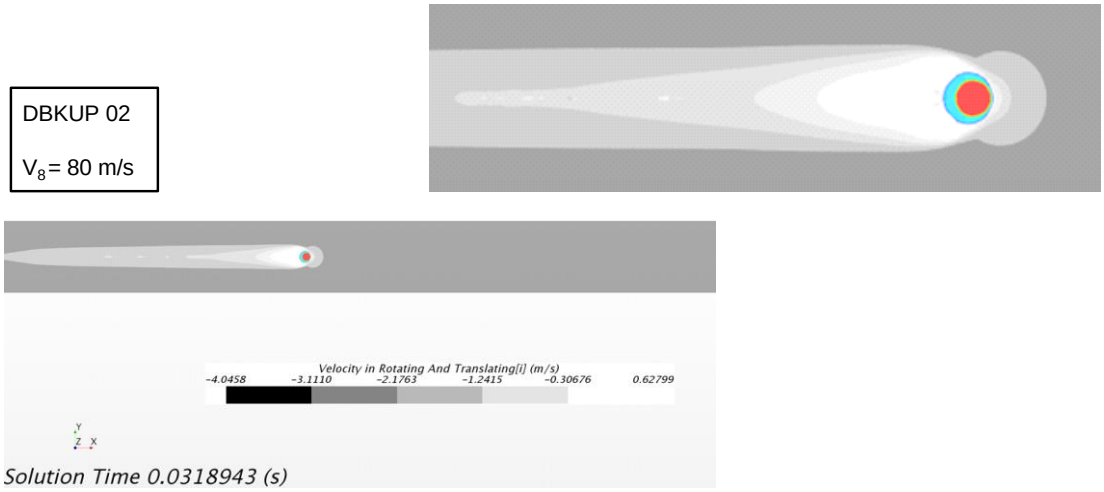

Figure 12: View of 473 µm Droplet Near the Start of Simulation Approaching DBKUP 02 Section

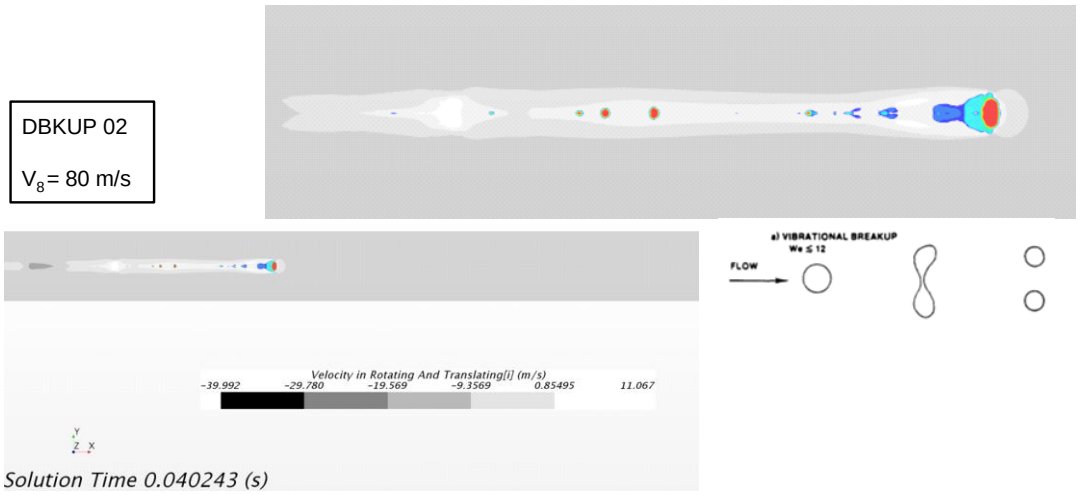

Figure 13: Onset of Vibrational Breakup (473 µm Droplet, DBKUP 02 Section) – Breakup Mechanism Image Taken from Pilch and Erdman[10]

Figure 14 shows more advanced breakup. In this figure, it is clear that mass has been torn away from the droplet without actually breaking up the core of the droplet. This is unexpected behavior. The relatively small size of droplets makes it difficult to pull mist off the surface of the droplet. The simulated behavior here is likely a result of a deficiency in the method. Namely, grid resolution may not be high enough, or with transverse deformation constrained, water that would have flowed into two separate lobes is instead peeled away into the airflow.

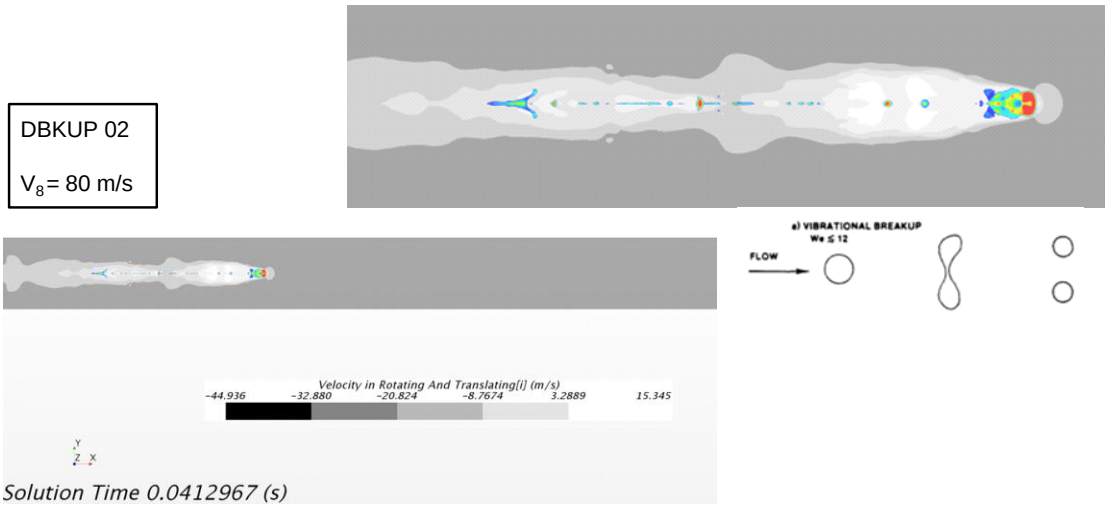

Figure 14: Vibrational Breakup Escalates (473 µm Droplet, DBKUP 02 Section) – Breakup Mechanism Image Taken from Pilch and Erdman[10]

Moments later a different behavior emerges. In Figure 15, the droplet flattens into a pancake shape signaling the onset of bag breakup. This is the first approximately axially symmetric breakup mode. Again, keep in mind that the figures only show a cross section of the droplet. To imagine the three-dimensional shape of the droplet, apply axisymmetry and revolve the droplet around its central axis.

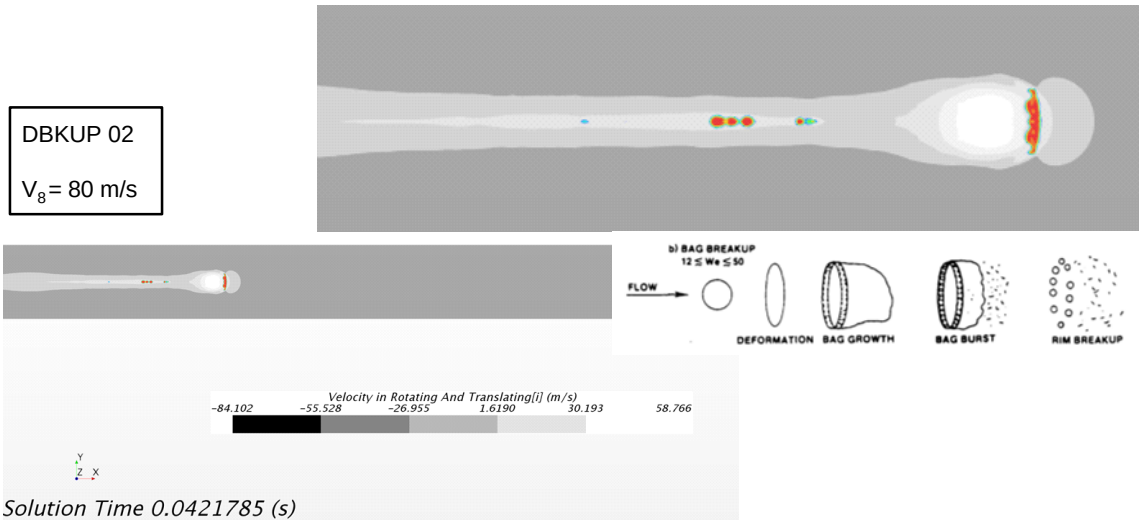

Figure 15: Onset of Bag Breakup(473 µm Droplet, DBKUP 02 Section) – Breakup Mechanism Image Taken from Pilch and Erdman[10]

Figure 16 depicts a fully formed bag. Here the droplet is significantly deformed into a sort of jellyfish shape. This shape is inherently unstable, and moments later as the top of the bag begins to pinch around the corners, the bag tears. This can be observed in Figure 17. Note in the close up view how the surface is no longer continuous. The tearing continuous down to the toroidal rim of the droplet. In previous experiments[10,17] analysis of bag breakup has shown that the majority of the fluid in the droplet is contained within the toroidal rim, and its decomposition is the most critical element in determining the resulting size of the water droplets. The toroid does not appear to have the same amount of fluid as what would be expected, but in its curled edge, there remains a significant amount of water. Note that while the tear in the droplet originates in the bag, but travels through the legs of the bag into the toroidal rim before the entire droplet breaks apart. Now with higher surface energy, the resulting droplet fragments will reform into smaller, rounder droplets.

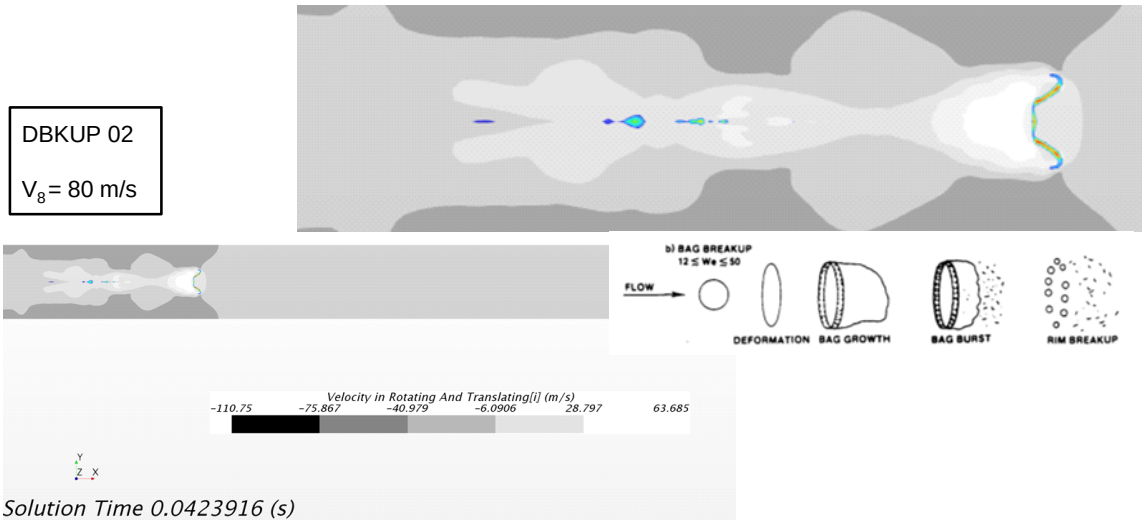

Figure 16: Full Bag Formation (473 µm Droplet, DBKUP 02 Section) – Breakup Mechanism Image Taken from Pilch and Erdman[10]

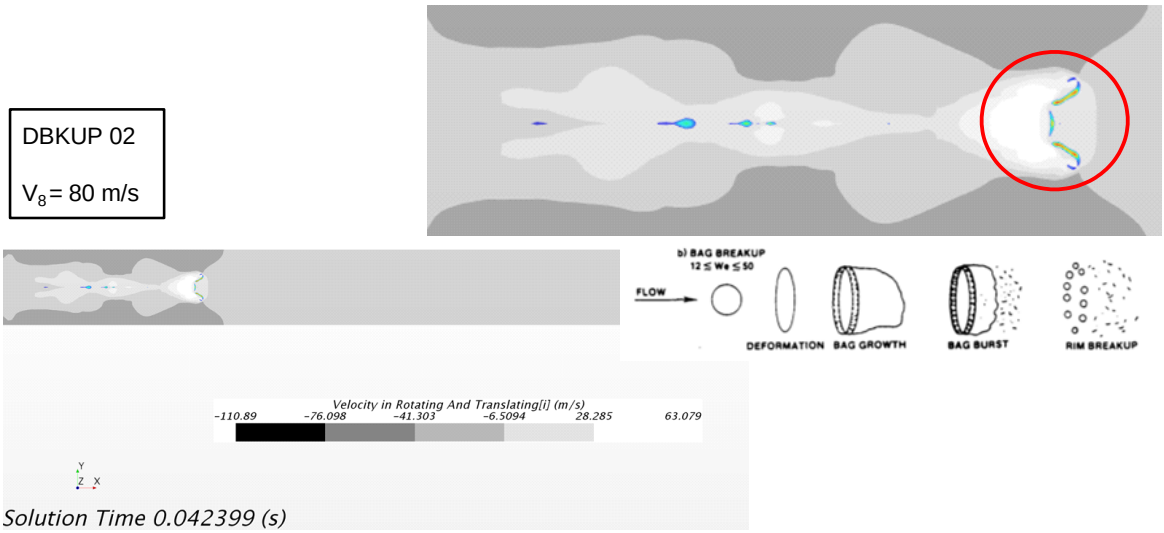

Figure 17: Initiation of Bag Breakup(473 µm Droplet, DBKUP 02 Section) – Breakup Mechanism Image Taken from Pilch and Erdman[10]

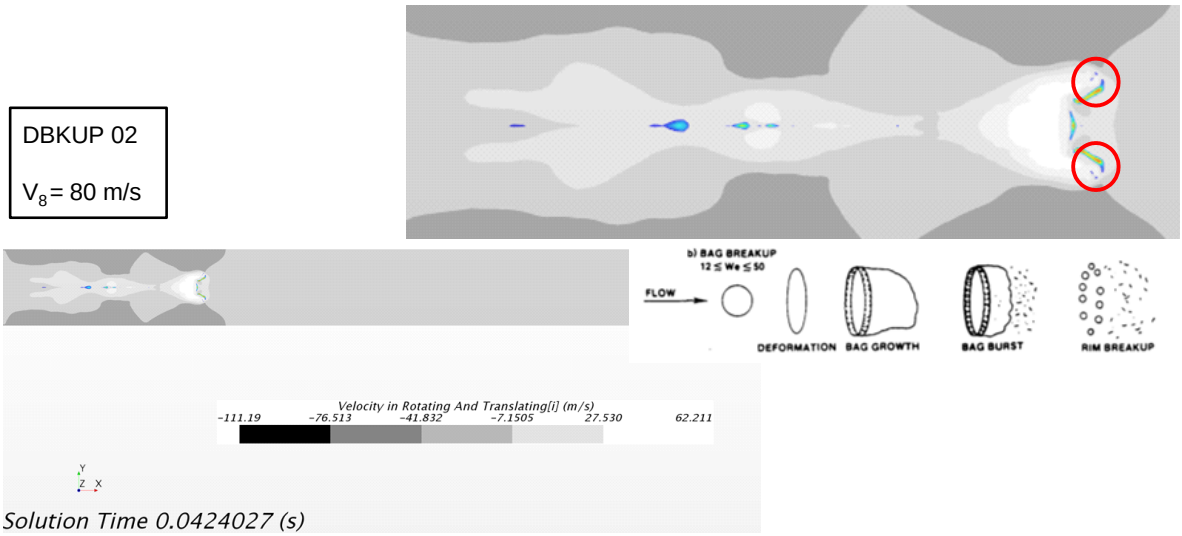

Figure 18: Collapse of Toroidal Rim (473 µm Droplet, DBKUP 02 Section) – Breakup Mechanism Image Taken from Pilch and Erdman[10]

The times from each of these captures was used to locate the value of *We* from the streamline data. Figure 19 shows where the last four scenes occurred and their corresponding Weber Numbers. This demonstrates that changing Weber Number Regime impacts the breakup mechanism of the droplet. The author cautions the reader that these values are slightly misleading. Mass has been extracted from the droplet over the path of travel, and thus the effective diameter of the droplet has been changing, thereby effecting the value for Weber Number, but insofar as Weber Number regimes exist for gradually accelerated droplets, Figure 19 demarks when along the droplets path does it reach critical points of stability. Note that the offset time has been subtracted away from the total time of the simulation to agree with the timestamps from the previous figures.

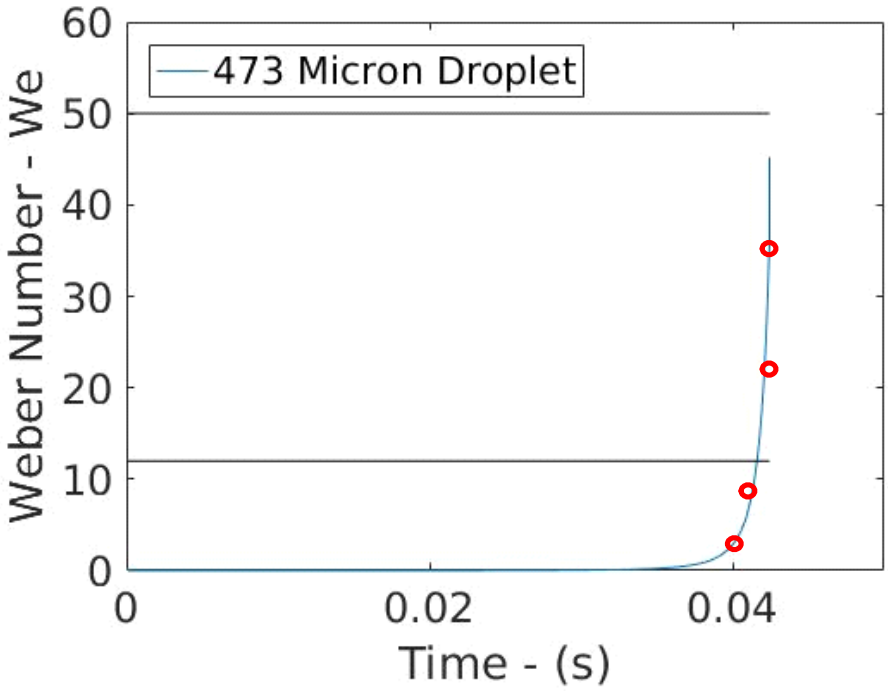

Figure 19: Weber Number of Previous Figures vs. Time Along Streamline

3.4: Results in Full

The remaining results of the numerical experiment are cataloged below. Each droplet that experienced breakup did so by following one of the mechanisms discussed in prior droplet breakup literature. The test conditions and results are arranged horizontally for each test. Breakup Time was read off of the simulations physical time, and then whatever offset time was used to ensure stability at the start of the test was added to it. The breakup mode was recorded as well.

Freestream Velocity (m/s)	Droplet Size (microns)	Airfoil	Breakup Time (s)	Critical Weber Number	Breakup Mode
100	50	NACA 0012	N/A	N/A	Did Not Breakup
100	100	NACA 0012	N/A	N/A	Did Not Breakup
100	200	NACA 0012	N/A	N/A	Did Not Breakup
80	473	DBKUP 02	0.040243	~9	Vibrational & Bag
120	2000	DBKUP 02	0.00297784	~12	Bag & Bag

Table 2: Table of Results

Chapter 4

Conclusion

Previous research has made massive strides in simulation capability. Different methodologies have been used with great success in predicting ice accretion. Supercooled Large Droplets pose a different kind of problem. Their large diameters complicate the physics of multiphase flow, and put old assumptions into question. Current tools for modeling these droplets still rely on experimental data that is, perhaps, less definitive than researchers consider it to be. This work outlines a strategy for investigating droplet dynamics at the individual droplet level. Reference frame shifts are applied to sequentially narrow the frame of view (and computational cost) down to a level that makes observations of small-scale behavior possible. Five proof of concept simulations were executed using this methodology. There results agree fairly well with existing theory (thus negating their need); however, variation remains large. Further study may be able to isolate droplets further and better represent the complex nature of droplet-entrained flows. Specifically, a model capable of resolving the small scales of the multi-phase interface could shed light on what causes the variation in Critical Weber Number. In addition, a high fidelity simulation could locate sub-breakup mechanisms that feed into the existing breakup mechanism but affect important output quantities such as resulting droplet diameter. Ice accretion is an incredibly complicated process and Supercooled Large Droplets complicate the process further by introducing a new world of physics to model. This work attempts to provide a means for investigating the complicated physics of droplet dynamics at the single droplet level.

BIBLIOGRAPHY

1. Rosenfeld, D. & Woodley, W. L. Deep convective clouds with sustained supercooled liquid water down to -37.5 degrees C. *Nature* **405,** 440–442 (2000).

2. Cober, S. G., Isaac, G. a. & Strapp, J. W. Characterizations of Aircraft Icing Environments that Include Supercooled Large Drops. *J. Appl. Meteorol.* **40,** 1984–2002 (2001).

3. Politovich, M. K. Aircraft Icing Caused by Large Supercooled Droplets. *J. Appl. Meteorol.* **28,** 856–868 (1989).

4. Papadakis, M. Computational Study of Large Droplet Breakup in the Vicinity of an Airfoil. 1–72 (2005).

5. SMITH, W. L. WEATHER PROBLEMS PECULIAR TO THE NEW YORK-CHICAGO AIRWAY. *Mon. Weather Rev.* **57,** 503–506 (1929).

6. Anonymous. *Annual report of the National Advisory Committee for Aeronautics (15th).administrative report including Technical Reports nos. 309 to 336*. (1929).

7. Wright, W. User's Manual for LEWICE Version 3.2. *Nasa/Cr-2008-214255* (2008). doi:20080048307

8. Kim, I., Bachchan, N. & Peroomian, O. Supercooled Large Droplet Modeling for Aircraft Icing Using an Eulerian–Eulerian Approach. *J. Aircr.* **53,** 487–500 (2015).

9. Dukowicz, J. K. A particle-fluid numerical model for liquid sprays. *J. Comput. Phys.* **35,** 229–253 (1980).

10. Pilch, M. & Erdman, C. A. Use of breakup time data and velocity history data to predict the maximum size of stable fragments for acceleration-induced breakup of a liquid drop. *Int. J. Multiph. Flow* **13,** 741–757 (1987).

11. Komabayasi, M., Gonda, T. & Isono, K. Life Time of Water Drops before Breaking Droplets * and Size Distribution of Fragment (Manuscript received 17 July 1964) Abstract Life times of water drops before breaking suspended freely in a vertical air stream have been empirically determined as a f. *J. Meteorol. Soc. Japan. Ser. II* **42,** 330–340 (1964).

12. Veras-Alba, B., Palacios, J., Vargas, M., Ruggeri, C. & Bartkus, T. P. Mechanism of Water Droplet Breakup near the Leading Edge of an Airfoil. 1–26 (2012). doi:doi:10.2514/6.2012-3129

13. Tan, S. C. & Papadakis, M. Parametric Experiment of Large Droplet Dynamics. (2007). doi:10.4271/2007-01-3346

14. Reitz, R. D. Modeling atomization processes in high-pressure vaporizing sprays. *At. Sprays* **3,** 309–337 (1987).

15. O'Rourke, P. J. & Amsden, A. A. The TAB Method for Numerical Calculation of Spray Droplet Breakup. (1987).

16. Spalart, P. R. & Allmaras, S. R. A one equation turbulence model for aerodynamic flows. *Rech. Aerosp. Ed.* 5 (1994).

17. Jain, M., Prakash, R. S., Tomar, G. & Ravikrishna, R. V. Secondary breakup of a drop at moderate Weber numbers. *Proc. R. Soc. A Math. Phys. Eng. Sci.* **471,** 20140930–20140930 (2015).

Jason E. Turner

Education ***Pennsylvania State University***, 2013 to 2017
Penn State Millennium Scholar
Schreyer Honors Scholar
Majors: B.S. Aerospace Engineering with Honors;
B.S. Engineering Science with Honors.

Special Coursework:

- E SC 407H - Computer Methods in Engineering Science.
  Programming intensive course that covers numerical methods for a variety of engineering applications including the finite element method and the finite difference method.
- MATH 412 - Fourier Series and Partial Differential Equations
  Orthogonal systems and Fourier series; derivation of some fundamental equations from mathematical physics, classification of partial differential equations; eigenvalue function method and its applications.
- MATH 441 - Matrix Algebra
  Rigorous Analysis of determinants, matrices, linear equations, characteristic roots, quadratic forms, and vector spaces.
- ME 524 - Turbulence and Applications to CFD: LES and DNS
  Scalings, decompositions, turbulence equations; scale representations, Direct and Large-Eddy Simulation modeling; pseudo-spectral methods;
- AERSP 412 - Turbulent Flow
  Fundamentals of turbulent flow, homogenous turbulence, spectral transfer of energy, viscous dissipation.
- AERSP 423 - Numerical Methods in Fluid Mechanics
  Finite difference methods applied to solving viscid/inviscid fluid dynamics problems, error control, numerical stability.

Programming Languages: MATLAB and C++

Research Experience ***Honors Thesis****, Applied Research Laboratory-Penn State*, Fall 2016 to 2017
"AN EVALUATION OF COMPUTATIONAL METHODS TO MODEL LARGE DROPLET BREAKUP"

Modeling Large Droplet Dynamics using Computational Fluid Dynamics (CFD)

- Examination on the effect of Weber number on breakup mechanism
- Simulation retrieves variable boundary conditions from steady Dispersed Multiphase RANS solution around airfoil and feeds into highly refined VOF droplet region.

Idaho National Laboratory, Summer 2015
Conducted Multi-Physics Modeling for Nuclear Waste Treatment Processes

- Model built with STAR-CCM+ and features Multi-Phase Flow, Ohmic Heating, and Heat Transfer models. Model informed waste treatment process decisions at The Hanford Nuclear Waste Treatment Plant.
- Constructed an artistic representation of my model that won 2nd place of 300 interns in the Sci-Art contest at the lab.
- Presented research at Schreyer Honors College "Scones and Scholars" student lecture series

Sailplane Laboratory, Fall 2013 to present
Designing and Constructing Human Powered Aircraft for Kremer Prize.

- Eight semester course sequence focusing on developing advanced understanding of aircraft design, stability and control, structures, and composite manufacturing techniques with both hands on lab work, and conceptual lectures
- Requires 2-3 comprehensive technical reports per semester.

Penn State Design Build Fly (DBF), Fall 2016 to Present
Designing Competition sponsored by AIAA

- Designing, building and flying small fixed wing electric model aircraft capable of fitting within a watertight, drop resistant tube and then deploying into a flight configuration.
- As a member my task is to assist with the mission analysis, specifically examining how different aircraft configurations would perform relative to others.
- I have also lead the design including: control surface sizing, structural configuration and systems integration.
- As the team leader I create group member schedules; I draft weekly agendas detailing current project status, upcoming deadlines and lessons learned; I manage the ordering of materials and group assignments; I coordinate with other sailplane class members and advisors helping us complete aircraft construction

---

Leadership Experience	Eagle Scout	Boy Scouts of America
	Academic Tutor and Mentor	Millennium Scholars Program
	Group Leader	Penn State DBF
	Millennium Scholars Program	Program Advisor